

Commun. Theor. Phys. **76** (2024) 055301 (8pp) https://doi.org/10.1088/1572-9494/ad3437

Investigating the impact of the universal function of the nuclear proximity potential in heavy-ion fusion cross sections

R Gharaei[1,2] **and E Sarvari**[3]

[1] Department of Physics, Sciences Faculty, Hakim Sabzevari University, PO Box 397, Sabzevar, Iran
[2] Department of Physics, Faculty of Science, Ferdowsi University of Mashhad, PO Box 91775-1436, Mashhad, Iran
[3] Science Faculty, Department of Physics, Tarbiat Modares University, Tehran, Iran

E-mail: r.gharaei@hsu.ac.ir

Received 7 January 2024, revised 12 March 2024
Accepted for publication 15 March 2024
Published 17 April 2024

Abstract

The fusion barriers and cross sections of 15 colliding systems with $320 \leqslant Z_1Z_2 \leqslant 1512$ are investigated in detail to understand the influence of the universal function of proximity potential formalism in the heavy-ion fusion mechanism. To realize this goal, we select three versions of the phenomenological proximity potentials, including Prox. 77, Zhang 2013, and Guo 2013, to calculate the nucleus–nucleus potential. The experimental fusion cross sections for the selected reactions are analyzed using the standard coupled-channel calculations, including couplings to the low-lying 2^+ and 3^- states in the target and projectile. The calculated results show that the universal functions of the Guo 2013 and Prox. 77 models provide the lowest and highest fusion barriers, respectively. In addition, it is found that the height of the fusion barriers is enhanced by increasing the mass number of the projectile from light to heavy ones. The highest sensitivity to the mass number of the projectile belongs to the results of Prox. 77. A discussion is also presented on the influence of the universal function on the radial behavior of the interaction potential in the allowed region for overlapping configurations. Our results reveal that the best fit to the experimental data of the fusion cross sections for the reactions involving light and medium nuclei is obtained using the universal function of the Zhang 2013 model. For the heavier systems, the results of the Guo 2013 model at sub-barrier energies provide a good description of the available data.

Keywords: fusion reactions, proximity-type potentials, universal function, coupled-channel calculations

(Some figures may appear in colour only in the online journal)

1. Introduction

Understanding the nucleus–nucleus potential is extremely crucial when analyzing the dynamics of heavy-ion fusion reactions. This potential is separated as the sum of the short-range attractive nuclear part and the long-range repulsive Coulomb force. Due to the strong competition between these two forces a Coulomb barrier appears in front of the participant nuclei. It is evident that in order for a fusion reaction to take place, the incident nucleus must have enough energy to overcome or penetrate the Coulomb barrier. The Coulomb component of the ion–ion potential is well recognized. Therefore, the main remaining task is to find an optimum form for calculating the nuclear part of the interaction potential precisely. Great theoretical efforts are in progress to describe the nuclear interactions using a wide range of fusion systems from light colliding pairs to heavy ones. The liquid-drop model [1, 2], double-folding model [3, 4], Woods–Saxon potential [5, 6], Skyrme energy-density [7], and the density-constrained time-dependent Hartree–Fock method

[8–10] are examples of applied theoretical approaches that are used to estimate the strength of nuclear interaction during the fusion process. The proximity potential formalism [11] is another theoretical approach used to deal with heavy-ion fusion reactions. It is generally based on the proximity force theorem [11, 12], according to which the nuclear part of the interaction potential can be taken as the product of two factors: one is dependent on the geometry of the reacting nuclei, and the other is the universal function that depends only on the separation distance of the reacting surfaces. From the literature, the original version of the proximity potential 1977 (Prox. 77) [11] fails to reproduce the experimental barrier heights satisfactorily [13–15]. Several improvements and modifications have been formulated in recent years concerning the formalism of the Prox. 77 model. The developments include the following [15–20]: a better form of the surface energy coefficient, a new parameterization for the nuclear radius, the introduction of an improved form of the universal function, or another parameterization for the surface thickness parameter. The last versions of the proximity potential formalisms are the Zhang 2013 and Guo 2013 models [18, 19]. It must be noted that the main difference between these two theoretical approaches lies in their universal function. It is shown that the results obtained from the Zhang 2013 and Guo 2013 potentials are in good agreement with the experimental data.

The focal task of the theoretical studies is to compute the fusion cross sections for different colliding systems in terms of the center-of-mass energies and to test their validity in comparison with the corresponding experimental data. It is well known that heavy-ion fusion at energies near and below the Coulomb barrier is a sensitive tool to evidence the influence of nuclear structure on reaction dynamics. From a theoretical point of view, the one-dimensional barrier penetration model (1D-BPM) is the simplest approach for describing the fusion process. Within the framework of this approach, the relative distance between the center-of-mass of two colliding nuclei is the only degree of freedom, and thus both the projectile and the target can be assumed to be structureless. From the literature [21, 22], one can find that the 1D-BPM successfully explains the experimental fusion data of light nuclei. For heavier systems, it works rather well at near and above-barrier energies but underestimates the sub-barrier fusion cross sections. In fact, numerous theoretical and experimental evidence indicates that the sub-barrier fusion cross sections for different colliding systems are severely enhanced over the predictions of the 1D-BPM [23–26]. It is clear from the existing reports that the coupling of various internal degrees of freedom, such as the coupling of low-lying inelastic excitations of interacting partners and transfer channels [27, 28], with the relative motion could be responsible for the enhancement of the sub-barrier fusion cross section. The coupled-channel (CC) calculations allow us to calculate the theoretical values of the fusion cross sections by including a strong coupling between the relative motion of colliding nuclei and the intrinsic degrees of freedom. These calculations transform the one-dimensional single barrier into multiple potential barriers and subsequently reduce the strength of the original barrier. The CC calculations can be performed by using the computer code CCFULL [29]. This code solves CC equations by imposing the incoming wave boundary conditions and allows us to include a finite number of rotational and vibrational states in both target and projectile nuclei.

In recent decades, many attempts have been made to describe the fusion process of two colliding nuclei using the proximity potential formalisms. The obtained results indicate that this theoretical approach needs to be modified. This is especially true for the fusion cross sections at energies below the Coulomb barrier. According to the differences between universal functions in the Prox. 77, Zhang 2013, and Guo 2013 potential models, we plan to systematically analyze the influence of this quantity by including the coupling to the low-lying inelastic excitations on the sub-barrier fusion cross sections. To realize this goal, an effort is made, using the standard CC formalism, to investigate 15 different projectile–target combinations with a focus on projectile mass. We consider the fusion of ^{28}Si, ^{36}S, ^{48}Ti, ^{64}Ni, and ^{86}Kr projectiles with the different target nuclei whose the mass numbers range from 58 to 208. This article is organized as follows. In section 2, the method for calculating the nucleus–nucleus potential within the framework of the different potential models is shown. The calculated results are presented and discussed in section 3. In section 4, the main conclusions of the present study are given.

2. Theoretical framework

The total interaction potential $V_{\rm T}(r)$ for spherical interacting nuclei with frozen densities can be written as

$$V_{\rm T}(r) = V_{\rm N}(r) + V_{\rm C}(r), \tag{1}$$

where r is the separation distance between the center-of-mass of the projectile and target nuclei. The Coulomb potential $V_{\rm C}(r)$ is written as

$$V_{\rm C}(r) = Z_1 Z_2 e^2 \begin{cases} \dfrac{1}{r}, & \text{for } r > r_C, \\ \dfrac{1}{2r_C}\left[3 - \left(\dfrac{r}{r_C}\right)^2\right], & \text{for } r < r_C, \end{cases} \tag{2}$$

where Z_1 and Z_2 are the proton numbers of the projectile and target nuclei. In this relation, the parameter r_C reads as $r_C = C_1 + C_2$ [14]. According to the proximity force theorem [11], '*the force between two gently curved surfaces in close proximity is proportional to the interaction potential per unit area between the two flat surfaces*'. Using the original version of the Prox. 77 , the nuclear part of the interaction potential between two reacting nuclei can be written as [13, 14]

$$V_p(r) = 4\pi\gamma b\overline{R}\,\Phi\left(\frac{s}{b}\right), \tag{3}$$

where the distance between near surfaces of the fragments $s = r - C_1 - C_2$. In addition, the mean curvature radius $\overline{R}$ can

be written as

$$\overline{R} = \frac{C_1 C_2}{C_1 + C_2}. \quad (4)$$

The Süsmann central radii of the fragments are given by

$$C_i = R_i\left[1 - \left(\frac{b}{R_i}\right)^2 + ...\right], \quad i = 1, 2. \quad (5)$$

Here, b is the surface width and was taken to be of the order of 1 fm. In addition, R_i is the effective sharp radius, which is given by

$$R_i = 1.28A_i^{1/3} - 0.76 + 0.8A_i^{1/3}, \quad i = 1, 2. \quad (6)$$

The dimensionless universal function $\Phi(\xi = s/b)$ was parameterized with the following form

$$\Phi(\xi) = \begin{cases} -\frac{1}{2}(\xi - 2.54)^2 - 0.0852(\xi - 2.54)^3, \\ \quad \text{for } \xi \leqslant 1.2511, \\ -3.437\exp(-\xi/0.75), \\ \quad \text{for } \xi \geqslant 1.2511. \end{cases} \quad (7)$$

In equation (3), γ refers to the nuclear surface tension coefficient and is given by the following equation

$$\gamma = \gamma_0\left[1 - k_s\left(\frac{N - Z}{N + Z}\right)^2\right], \quad (8)$$

where N and Z are neutron and atomic numbers of the parent nuclei, respectively. In this relation, γ_0 and k_s are the surface energy and surface asymmetry constants, respectively. For the Prox. 77 proximity potential, these constants were parameterized as $\gamma_0 = 0.9517$ MeV. fm^{-2} and $k_s = 1.7826$. In 2013 [19], Guo *et al* introduced a modified form of the nucleus–nucleus potential by analyzing the universal function of the proximity potential within the framework of the double-folding model for several hundreds of fusion reactions. Zhang *et al* [18] made a similar effort with the universal function of the proximity potential between the alpha and daughter nuclei by systematically analyzing the different parent nuclei with $Z = 48 - 92$. The authors of [18] parameterized a new formula for the universal function of the proximity potential as

$$\Phi(\xi) = \frac{p_1}{1 + \exp\left(\frac{\xi + p_2}{p_3}\right)}, \quad (9)$$

where the parameters (p_1, p_2, p_3) are equal to (−7.65, 1.02, 0.89) and (−17.72, 1.30, 0.854) for the Zhang 2013 and Guo 2013 proximity potentials, respectively. Finally, it must be noted that the mean curvature radius $\overline{R}$ of the nuclear reaction system in these proximity versions is defined as $\frac{R_1 R_2}{R_1 + R_2}$ instead of $\frac{C_1 C_2}{C_1 + C_2}$ in equation (4). Therefore, it will be interesting to see whether this change in the definition of the $\overline{R}$ parameter significantly affects the calculations of the nucleus–nucleus potential and thus fusion cross sections. Indeed, the comparison of the results obtained from the $\frac{C_1 C_2}{C_1 + C_2}$ definition with the $\frac{R_1 R_2}{R_1 + R_2}$ results provides the possibility to look for the role of the mean curvature radius parameter in the fusion process of two heavy ions.

Table 1. The selected categories of projectile–target combinations. The fusion systems are listed with respect to their increasing A_1A_2 values.

Category	Projectile	Target
Category 1	^{28}Si	^{62}Ni, ^{92}Zr, ^{208}Pb
Category 2	^{36}S	^{48}Ca, ^{90}Zr, ^{100}Mo
Category 3	^{48}Ti	^{58}Ni, ^{64}Ni, ^{122}Sn
Category 4	^{64}Ni	^{64}Ni, ^{92}Zr, ^{114}Sn
Category 5	^{86}Kr	^{70}Ge, ^{76}Ge, ^{100}Mo

3. Results and discussion

In the present work, we consider 15 heavy-ion fusion reactions, including the fusion of ^{28}Si, ^{36}S, ^{48}Ti, ^{64}Ni, and ^{86}Kr projectiles with different targets under the condition $48 \leqslant A \leqslant 208$ for their mass numbers. Our selected reactions are presented in table 1 as five categories of the projectile–target combinations. We use the Zhang 2013 and Guo 2013 proximity potential models to calculate the total interaction potential in different colliding systems. According to [19], the precision of the Guo 2013 proximity potential has only been tested for Coulomb barrier parameters. However, we emphasize that the fusion cross section is the most important observable in heavy-ion fusion reactions. Meanwhile, as stated earlier, the Zhang 2013 model has been introduced based on the analysis of the alpha-decay process. However, the results of the previous studies reveal that a definite potential model can be appropriate to describe both alpha-decay and fusion processes [30]. In this situation, the analysis of the validity of the Zhang 2013 and Guo 2013 proximity potentials for predicting the measured fusion cross sections will be a guide to future theories based on the proximity approach.

The purpose of this study is to analyze the influence of the nuclear structure effects, including coupling to the low-lying inelastic excitation 2^+ and 3^- of both target and projectile nuclei, on the heavy-ion fusion process. To realize our goal, the CC model has been used to estimate the theoretical values of the fusion cross sections. For comparison, the CC calculations based on the original version of the Prox. 77 are also considered to incorporate the nuclear structure effects. Since the main difference between these three versions of the proximity potential formalisms is in the universal function $\phi(s)$, the simultaneous comparison of the obtained results provides ideal conditions to investigate the role of the universal function of the nuclear proximity potential in the fusion of two colliding nuclei. However, as mentioned earlier, the definition of the mean radius parameter $\overline{R}$ in the formalism of the original version of the proximity potential is different from the Zhang 2013 and Guo 2013 models. Therefore, it would be interesting to analyze the influence of the use of the different definitions of the $\overline{R}$ parameter on the fusion of various combinations of the selected nuclei. In figure 1, the

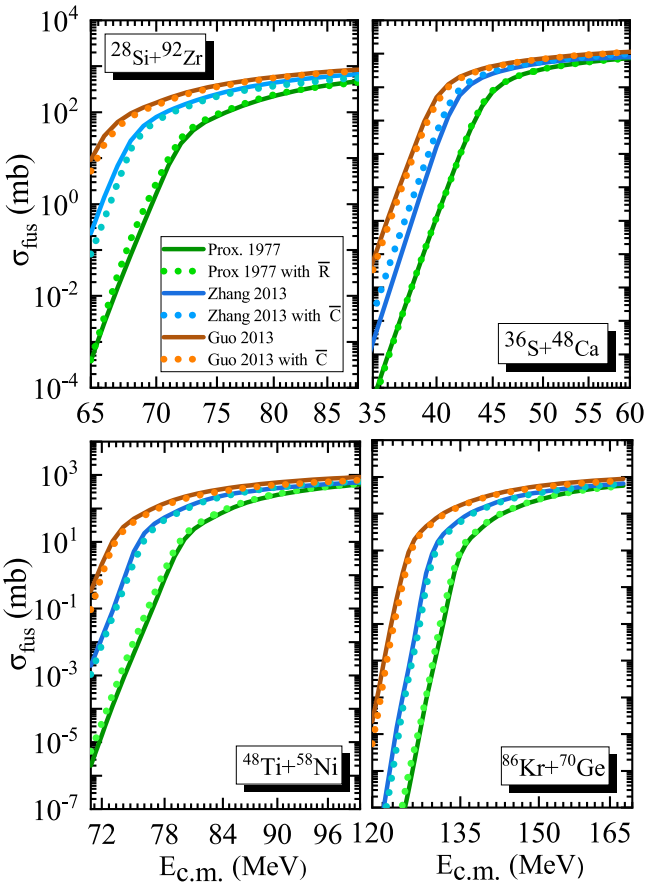

Figure 1. Comparison of the theoretical values of the fusion cross sections using the Prox. 77, Zhang 2013, and Guo 2013 proximity potentials with $\overline{R}$ and $\overline{C}$ calculations for the fusion reactions $^{28}\mathrm{Si} + {}^{92}\mathrm{Zr}$ (top left), $^{36}\mathrm{S} + {}^{48}\mathrm{Ca}$ (top right), $^{48}\mathrm{Ti} + {}^{58}\mathrm{Ni}$ (bottom left), and $^{86}\mathrm{Kr} + {}^{70}\mathrm{Ge}$ (bottom right).

experimental fusion cross sections are compared to several CC calculations that are based on the Prox. 77, Zhang 2013, and Guo 2013 proximity potentials with both definitions of the mean curvature radius $\overline{R}$ for four arbitrary reactions: $^{28}\mathrm{Si} + {}^{92}\mathrm{Zr}$, $^{36}\mathrm{S} + {}^{48}\mathrm{Ca}$, $^{48}\mathrm{Ti} + {}^{58}\mathrm{Ni}$, and $^{86}\mathrm{Kr} + {}^{70}\mathrm{Ge}$. In the calculation of the theoretical values of the fusion cross sections, we include couplings to the low-lying surface excitations of the projectile and target and also their collective couplings. The nuclear structure inputs for different colliding nuclei, including the quadrupole deformation β_2 and octupole deformation β_3 together with their excitation energies E_2 and E_3 for 2^+ and 3^- vibrational states, are tabulated in table 2. One can see that the change in the definition of the $\overline{R}$ parameter from $\frac{R_1R_2}{R_1+R_2}$ to $\frac{C_1C_2}{C_1+C_2}$ decreases the strength of the calculated fusion cross sections, especially at low energies. However, it is clear that the available fusion cross sections have very low sensitivity to the imposition of such effects. This means that the effects due to the difference in the above-mentioned definitions can be ignored.

3.1. The role of the universal function in the fusion barriers

By analyzing the radial behavior of the nuclear and total potentials based on the three considered proximity potential versions, rich knowledge of the influence of the universal function of the proximity potential on the heavy-ion fusion reactions can be achieved.

This situation is illustrated by the left and right panels of figure 2 for one of the fusion reactions existing in each of the five considered categories of the projectile–target combinations. Here, the distributions of the $V_T(r)$ (MeV) potential are presented as a function of the separation distance r (in fm) using the Zhang 2013, Guo 2013, and Prox. 77 models. One can see that only the original version of Prox. 77 produces a rather shallow pocket in the entrance channel potential. The two other forms of the interaction potentials are unrealistic at a distance smaller than the touching configuration of the colliding pairs, where they provide pockets in the entrance channel potential that are far too deep. However, one can conclude that the potentials calculated by Guo 2013 are found to be far more attractive than Zhang 2013. The physical justification for the observed behavior in all the reaction systems comes from the analysis of the calculated universal functions as a function of the separation distance between the

Table 2. The values of the excitation energies E^* (in MeV) and the corresponding deformation parameters β^λ of low-lying 2^+ and 3^- states used in the CC calculations for the selected nuclei. The values are extracted from [31, 32].

Nucleus	λ^π	E^*(MeV)	β^λ
^{28}Si	2^+	1.779	0.4082
	3^-	6.879	0.401
^{36}S	2^+	3.2909	0.1569
	3^-	4.193	0.376
^{48}Ca	2^+	3.8317	0.1054
	3^-	4.507	0.23
^{48}Ti	2^+	0.9835	0.2575
	3^-	3.359	0.197
^{58}Ni	2^+	1.4542	0.1768
	3^-	4.475	0.198
^{62}Ni	2^+	1.1729	0.1969
	3^-	3.757	0.197
^{64}Ni	2^+	1.3458	0.1702
	3^-	3.56	0.201
^{70}Ge	2^+	1.0395	0.2264
	3^-	2.561	0.274
^{76}Ge	2^+	0.5629	0.265
	3^-	2.692	0.144
^{86}Kr	2^+	1.5648	0.1347
	3^-	3.099	0.149
^{90}Zr	2^+	2.1863	0.211
	3^-	2.748	0.1569
^{92}Zr	2^+	0.9345	0.1
	3^-	2.34	0.174
^{100}Mo	2^+	0.5356	0.234
	3^-	1.908	0.218
^{114}Sn	2^+	1.2999	0.1147
	3^-	2.275	0.134
^{122}Sn	2^+	1.1405	0.1027
	3^-	2.493	0.121
^{208}Pb	2^+	4.0855	0.0541
	3^-	2.615	0.111

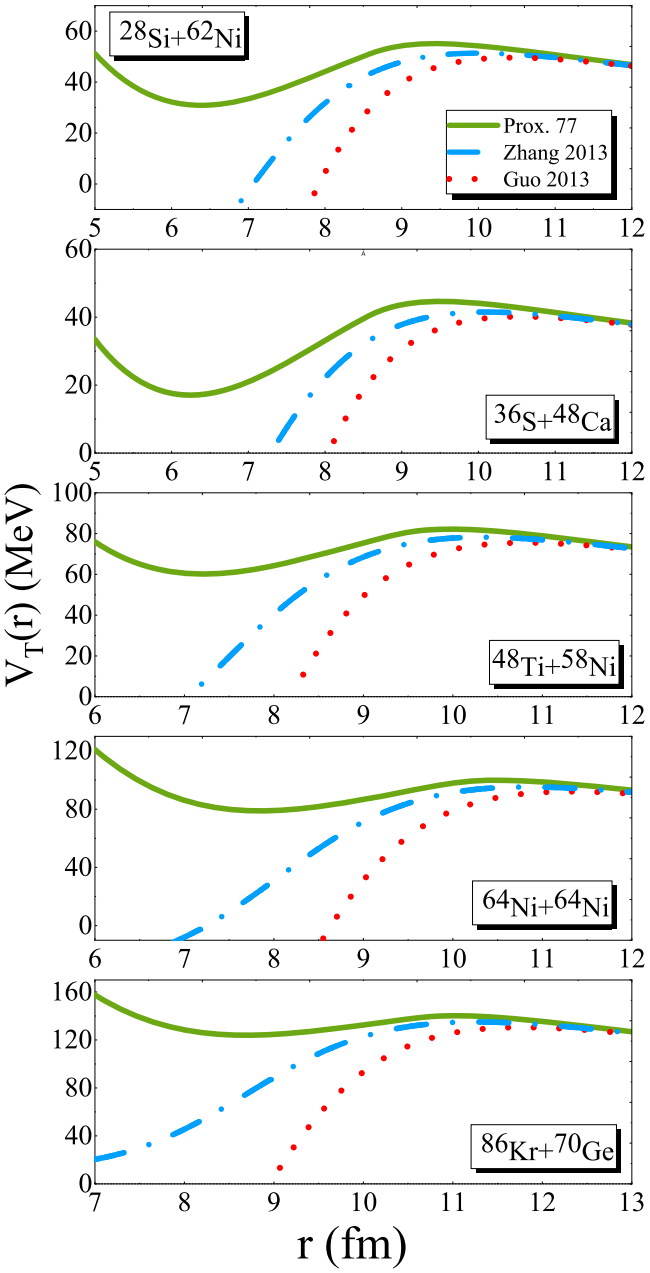

Figure 2. The radial distributions of the total interaction potential $V_T(r)$, including the three versions of the proximity potentials for different colliding systems.

surfaces of two colliding nuclei. This is because, according to equation (3), the nuclear potential $V_N(r)$ depends directly on the universal function $\Phi(s)$. A clear difference can be seen between the calculated universal functions from the different proximity potentials at shorter distances. Meanwhile, the data points maintain a similar tendency at a distance larger than the touching configuration of the colliding pairs.

From the results presented in figure 3, we see that the difference in the universal function leads to significant changes in the fusion barriers. It is observed that the height of the Coulomb barrier increases from the Guo 2013 to the Prox. 77 proximity potentials. To investigate the influence of the mass of the projectile on the fusion barriers, we are interested

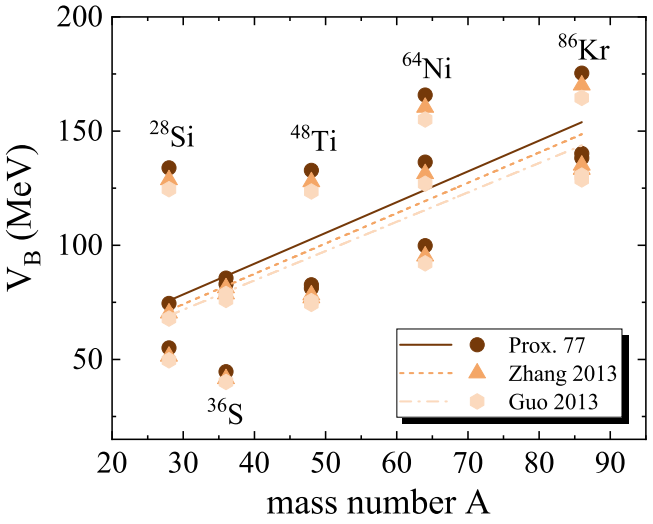

Figure 3. The variation trend of the fusion barrier heights calculated from the Prox. 77, Zhang 2013, and Guo 2013 proximity potentials as a function of the mass number of the projectiles for all five categories of the projectile–target combinations listed in table 1. The solid lines represent the linear behaviors of the data points.

in analyzing the behavior of the calculated barrier heights by increasing the mass number A of the projectile. The results for different versions of the proximity potentials are shown in figure 3. One can see that the values of V_B increase from light mass to heavy mass. In addition, the analysis of the linear trend of the obtained results indicates that the sensitivity of the Prox. 77 model to the change in the values of the mass number A is slightly greater than that of the other two models.

3.2. The role of the universal function in the fusion cross sections

Theoretically, the standard approach to study heavy-ion fusion cross sections is via the quantum tunneling through the relative barrier of the dinuclear system coupled to different low-lying collective degrees of freedom, such as vibrational and rotational excitations of the participating nuclei. The CC formalism is a useful method to describe the dynamics of the fusion process at sub-barrier bombarding energies. However, the authors typically employed the standard form of the Wong formula to calculate the theoretical values of the fusion cross sections within the framework of the proximity potential formalisms, see, for example [13–15]. In the present work, we perform the exact CC calculations for the selected reactions using the computer code CCFULL [29]. This code allows us to include a finite number of rotational and vibrational states in both interacting nuclei during fusion. The parameters used in the calculations of the fusion cross sections are presented in table 2. In figure 4, we display the fusion cross sections σ_{fus} (in mb) as a function of the center-of-mass energy $E_{c.m.}$ (in MeV) for the reactions existing in categories 1 to 5. It is shown that the original version of Prox. 77 substantially underestimates the fusion cross section at sub-barrier energies. This result indicates the importance of the barrier shape in the calculations of the fusion cross sections. In fact, as mentioned

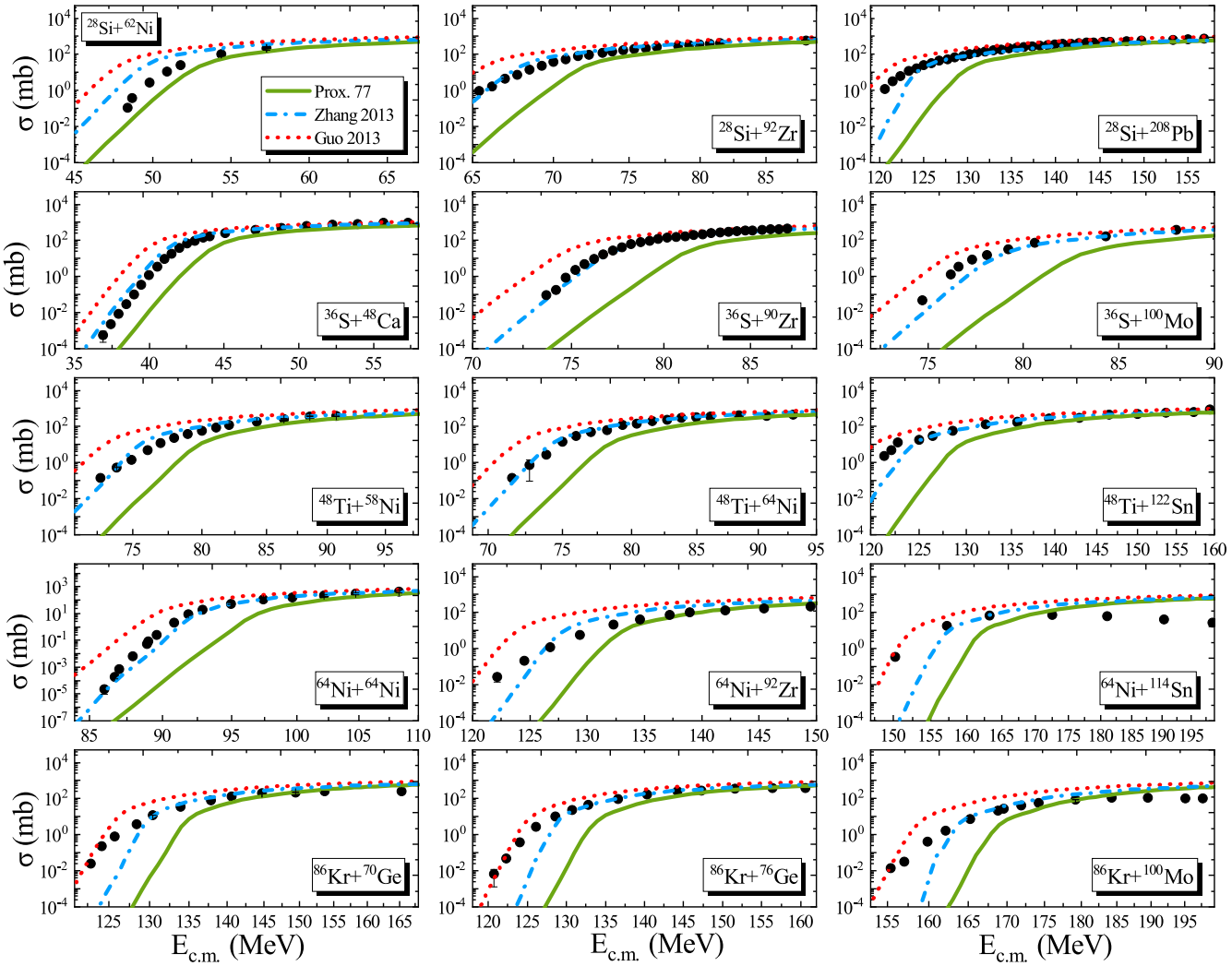

Figure 4. Experimental fusion excitation functions for the selected systems compared with various CC calculations based on the Prox. 77, Zhang 2013, and Guo 2013 proximity potentials.

before, the universal function of the Prox. 77 provides the highest values for the fusion barrier height. Although, it reproduces the experimental data well at energies above the Coulomb barrier for different colliding systems. To improve the fit to the fusion data, we can use the universal function of the Zhang 2013 and Guo 2013 proximity potentials. From the results presented in figure 4, one can find that an excellent fit to the experimental fusion cross sections is achieved for the CC calculations based on the universal function of the Zhang 2013 potential. This result holds true for categories involving light- and medium-mass projectile nuclei, namely ^{28}Si, ^{36}S, ^{48}Ti, and ^{64}Ni. Nevertheless, we see that the CC calculations based on the Zhang 2013 potential are suppressed at low energies when compared with the results of the Guo 2013 potential for heavier systems. Indeed, it appears from figure 4 that the universal function of the Guo 2013 proximity potential is appropriate for dealing with the fusion process of heavier projectiles that exist in category 5 and also the fusion process of different projectiles with heavy targets, including ^{208}Pb, ^{100}Mo, and ^{114}Sn in categories 1, 2, and 3, respectively.

4. Conclusion

To summarize, the influence of the universal function of the proximity potential on the fusion process of two heavy nuclei has been investigated using three different parameterizations within the proximity concept. We calculate the nuclear potential of 15 projectile–target combinations (with $320 \leqslant Z_1Z_2 \leqslant 1512$) based on the Prox. 77, Zhang 2013, and Guo 2013 proximity potentials. The calculations of fusion cross sections were performed using the standard CC approach by applying the effects of the low-lying nuclear structure in the projectile and target. The main conclusions of the present work can be summarized as follows.

- It is shown that the change in the definition of the mean curvature radius $\overline{R}$ from $\frac{C_1C_2}{C_1+C_2}$ to $\frac{R_1R_2}{R_1+R_2}$ and vice versa does not have a significant impact on the energy-dependent behavior of the fusion cross sections. This means that one can ignore the difference between the three considered proximity potentials from the perspective of the radius definition $\overline{R}$.

- The analysis of the influence of the universal function on the radial behavior of the nucleus–nucleus potential reveals that the universal functions based on the Zhang 2013 and Guo 2013 models lead to a very deep pocket in the entrance channel potential. Our analysis based on the different versions of the proximity potential formalisms shows that the calculated values of the fusion barrier heights increase from the Guo 2013 to the Prox. 77 approach. This result indicates the importance of the universal function of the nuclear proximity potential in the determination of the fusion probability.
- The sensitivity of the calculated fusion barrier heights to the change in the mass number of the projectile nuclei has systematically been investigated. The obtained results indicate that the values of V_B based on the three versions of the phenomenological proximity potentials follow an increasing trend with the increase in the mass number of the projectile from light to heavy nuclei. In addition, one can find that the results of the original version off Prox. 77 are more sensitive toward the mass number dependence.
- In the present study, the measured fusion cross sections for different selected systems have been compared with the results of CC calculations that are based on the Prox. 77, Zhang 2013, and Guo 2013 proximity potentials. The calculations were performed using the computer code CCFULL by considering the lowest quadrupole and octupole excitations in the projectile and target. It is shown that the original version of the universal function based on the Prox. 77 model apparently underestimates the fusion cross section for heavy-ion fusion reactions. It seems that the proximity formalism with the universal function of the Zhang 2013 model may be more appropriate for the fusion of light- and medium-mass nuclei in comparison with the heavy-mass nuclei. This theoretical approach underestimates the sub-barrier fusion cross sections for the heavier systems. The results of the calculations using the proximity concept with the universal function of the Guo 2013 approach were found to be in good agreement with the cross section measurements at low energies for fusion reactions involving heavy projectiles and/or targets.

ORCID iDs

R Gharaei https://orcid.org/0000-0003-2256-0028

References

[1] Royer G, Prince M, Scannell X, Lele-Cheudjou I and Samb A 2020 Fusion reactions and synthesis of some superheavy nuclei *Nucl. Phys.* A **1000** 121811
[2] Royer G, Guillot M and Monard J 2021 Fusion and fission barrier heights and positions within the Generalized Liquid Drop Model *Nucl. Phys.* A **1010** 122191
[3] Satchler G R and Love W G 1979 Folding model potentials from realistic interactions for heavy-ion scattering *Phys. Rep.* **55** 183
[4] Khoa D T and Satchler G R 2000 Generalized folding model for elastic and inelastic nucleus–nucleus scattering using realistic density dependent nucleon–nucleon interaction *Nucl. Phys.* A **668** 3
[5] Newton J O, Butt R D, Dasgupta M, Hinde D J, Gontchar I I and Morton C R 2004 Systematic failure of the Woods–Saxon nuclear potential to describe both fusion and elastic scattering: possible need for a new dynamical approach to fusion *Phys. Rev.* C **70** 024605
[6] Gontchar I I, Hinde D J, Dasgupta M and Newton J O 2003 Surface diffuseness of nuclear potential from heavy-ion fusion reactions *Nucl. Phys.* A **722** 479
[7] Vautherin D and Brink D M 1972 Hartree–Fock calculations with Skyrmes interaction. I. spherical nuclei *Phys. Rev.* C **5** 626
[8] Umar A S, Strayer M R, Cusson R Y, Reinhard P-G and Bromley D A 1985 Time-dependent Hartree–Fock calculations of ^{4}He. ^{14}C, ^{12}C + ^{12}C(0^{+}), and ^{4}He + ^{20}Ne molecular formations *Phys. Rev.* C **32** 172
[9] Umar A S and Oberacker V E 2006 Heavy-ion interaction potential deduced from density-constrained time-dependent Hartree–Fock calculation *Phys. Rev.* C **74** 021601(R)
[10] Umar A S and Oberacker V E 2006 Study of Ni-64 + Sn-132 fusion with density constrained TDHF formalism *Phys. Rev.* C **74** 061601(R)
[11] Blocki J, Randrup J, Swiatecki W J and Tsang C F 1977 Proximity forces *Ann. Phys.* **105** 427
[12] Blocki J and Swiatecki W J 1981 A generalization of the proximity force theorem *Ann. Phys.* **132** 53
[13] Dutt I and Puri R K 2010 Systematic study of the fusion barriers using different proximity-type potentials for N = Z colliding nuclei: new extensions *Phys. Rev.* C **81** 044615
[14] Dutt I and Puri R K 2010 Comparison of different proximity potentials for asymmetric colliding nuclei *Phys. Rev.* C **81** 064609
[15] Dutt I and Puri R K 2010 Role of surface energy coefficients and nuclear surface diffuseness in the fusion of heavy-ions *Phys. Rev.* C **81** 047601
[16] Ghodsi O N, Moshfegh H R and Gharaei R 2013 Role of the saturation properties of hot nuclear matter in the proximity formalism *Phys. Rev.* C **88** 034601
[17] Gharaei R, Kamelan Najjar F and Ghal-Eh N 2021 Systematic study on α-decay half-lives: a new dependency of effective sharp radius on α-decay energy *Eur. Phys. J.* A **57** 104
[18] Zhang G L, Zheng H B and Qu W W 2013 Study of the universal function of nuclear proximity potential between α and nuclei from density-dependent nucleon–nucleon interaction *Eur. Phys. J.* A **49** 10
[19] Guo C, Zhang G and Le X 2013 Study of the universal function of nuclear proximity potential from density-dependent nucleon–nucleon interaction *Nucl. Phys.* A **897** 54
[20] Dutt I and Bansa R 2010 A modified proximity approach in the fusion of heavy ions *Chin. Phys. Lett.* **27** 112402
[21] Hagino K and Takigawa N 2012 Subbarrier fusion reactions and many-particle quantum tunneling *Prog. Theor. Phys.* **128** 1061
[22] Vaz L C, Alexander J M and Satchler G R 1981 Fusion barriers, empirical and theoretical: evidence for dynamic deformation in subbarrier fusion *Phys. Rep.* **69** 373
[23] Bierman J D, Chan P, Liang J F, Kelly M P, Sonzogni A A and Vandenbosch R 1996 Experimental fusion barrier distributions reflecting projectile octupole state coupling to prolate and oblate target nuclei *Phys. Rev. Lett.* **76** 1587

[24] Hagino K, Takigawa N, Dasgupta M, Hinde D J and Leigh J R 1997 Adiabatic quantum tunneling in heavy-ion sub-barrier fusion *Phys. Rev. Lett.* **79** 2014
[25] Back B B, Esbensen H, Jiang C L and Rehm K E 2014 Recent developments in heavy-ion fusion reactions *Rev. Mod. Phys.* **86** 317
[26] Dasgupta M, Hinde D J, Rowlay N and Stefanini A M 1998 Measuring barriers to fusion *Annu. Rev. Nucl. Part. Sci.* **48** 401
[27] Montagnoli G *et al* 2018 Fusion hindrance for the positive Q-value system $^{12}C + ^{30}Si$ *Phys. Rev.* C **97** 024610
[28] Colucci G *et al* 2018 Isotopic effects in sub-barrier fusion of Si + Si systems *Phys. Rev.* C **97** 044613
[29] Hagino K, Rowley N and Kruppa A T 1999 A program for coupled-channel calculations with all order couplings for heavy-ion fusion reactions *Comput. Phys. Commun.* **123** 143
[30] Gharaeia R and Mohammadi S 2019 Study of the surface energy coefficient used in nuclear proximity potential of the α-nuclei systems from density-dependent nucleon–nucleon interactions *Eur. Phys. J.* A **119** 55
[31] Raman S, Nestor C W Jr. and Tikkanen P 2001 Transition probability from the ground to the first-excited 2^+ state of even-even nuclides *At. Data Nucl. Data Tables* **78** 1
[32] Spear R H 1989 Reduced electric-octupole transition probabilities, B (E3; $0_1^+ \rightarrow 3_1^-$), for even-even nuclides throughout the periodic table *At. Data Nucl. Data Tables* **42** 55